SIAM J. SCI. COMPUT.
Vol. 31, No. 4, pp. 2419–2446

CONSTRUCTION OF SIMPLE, STABLE, AND CONVERGENT HIGH ORDER SCHEMES FOR STEADY FIRST ORDER HAMILTON–JACOBI EQUATIONS*

R. ABGRALL†

Abstract. We develop a very simple algorithm that permits to construct compact, high order schemes for steady first order Hamilton–Jacobi equations. The algorithm relies on the blending of a first order scheme and a compact high order scheme. The blending is conducted in such a way that the scheme is formally high order accurate. A convergence proof without error estimate is given. We provide several numerical illustrations that demonstrate the effective accuracy of the scheme. The numerical examples use triangular unstructured meshes, but our method may be applied to other kind of meshes. Several implementation remarks are also given.

Key words. Hamilton–Jacobi, unstructured meshes, high order schemes

AMS subject classifications. 65M60, 35L60, 65M12, 49L25

DOI. 10.1137/040615997

1. Introduction.

We consider the following Cauchy problem: find $u \in C^0(\Omega)$, the space of continuous function on the open subset $\Omega \subset \mathbb{R}^d$ such that

$$\begin{aligned} H(x,u,Du) &= 0 \quad x \in \Omega \subset \mathbb{R}^d, \\ u &= g \quad x \in \partial\Omega, \end{aligned} \tag{1.1}$$

in the viscosity sense. In (1.1), $(x,s,p) \in \overline{\Omega} \times \mathbb{R} \times \mathbb{R}^d \mapsto H(x,s,p)$ is uniformly continuous.

Before going further, let us briefly review the notion of viscosity solution for (1.1). For any function z, we consider the upper semicontinuous (u.s.c.) and lower semicontinuous (l.s.c.) envelopes of z with respect to all the variables. They are defined by

$$z^*(x) = \limsup_{x \to y} z(y) \text{ and } z_*(x) = \liminf_{x \to y} z(y).$$

Following [1], we introduce the function G:

$$G(x,s,p) = \begin{cases} H(x,s,p) & x \in \Omega, \\ s - g(x) & x \in \partial\Omega. \end{cases}$$

The computation of G_* and G^* is easy, and we have

$$\begin{cases} G_*(x,s,p) = G^*(x,s,p) = H(x,s,p) & \text{if } x \in \Omega, \\ G_*(x,s,p) = \min(H(x,s,p), s - g(x)) & \text{if } x \in \partial\Omega, \\ G^*(x,s,p) = \max(H(x,s,p), s - g(x)) & \text{if } x \in \partial\Omega. \end{cases} \tag{1.2}$$

*Received by the editors September 30, 2004; accepted for publication (in revised form) January 23, 2009; published electronically June 12, 2009. This work was partially supported by SME, Saint Médard en Jalles, and E.U. RT Network Hyke HPRN-CT-2002-0282.
http://www.siam.org/journals/sisc/31-4/61599.html
†Mathématiques Appliquées de Bordeaux, Université Bordeaux I, 341 Cours de la Libération, 33 405 Talence Cedex, France (abgrall@math.u-bordeaux1.fr).

A locally bounded upper semicontinuous function u defined on $\overline{\Omega}$ is a viscosity subsolution of (1.1) if and only if, for any $\phi \in C^1(\overline{\Omega})$, if $x_0 \in \overline{\Omega}$ is a local maximum of $u - \phi$, then

$$G_*(x_0, u(x_0), D\phi(x_0)) \leq 0. \tag{1.3}$$

Similarly, u, a locally bounded, l.s.c. function defined on $\overline{\Omega}$ is a viscosity supersolution of (1.1) if and only if, for any $\phi \in C^1(\overline{\Omega})$, if $x_0 \in \overline{\Omega}$ is a local minimum of $u - \phi$, then

$$G^*(x_0, u(x_0), D\phi(x_0)) \geq 0. \tag{1.4}$$

A viscosity solution is simultaneously a subsolution and a supersolution of (1.1).

This can be generalized to other types of boundary conditions such as Neumann, etc.

Under standard assumptions on the open subset Ω, g, and H, one can prove existence and uniqueness of the viscosity solutions of (1.1); see [1]. In particular, this is true if the Hamiltonian H is convex in $p \in \mathbb{R}^d$ and if $\partial\Omega$ Lipschitz continuous.

In this paper, we assume that (1.1) has a uniqueness principle, that is, any subsolution u and any supersolution v of (1.1) satisfy

$$\forall x \in \Omega, \qquad u(x) \leq v(x).$$

Throughout the paper, we consider a family of regular triangulations. The triangulations are denoted by $\mathcal{T}^h$, h is the maximum diameter of the elements K_j, $j = 1, \ldots, n_e$, and $\{x_i\}_{j=1,\ldots,n_s}$ is the set of vertices of $\mathcal{T}^h$. The family of triangulations is also assumed to be shape regular, that is, there exist constants C_1 and C_2 such that the diameter of K_j satisfy

$$C_1 h \leq \operatorname{diam}(K_j) \leq C_2 h \qquad \forall j = 1, \ldots, n_e. \tag{1.5}$$

For a given triangulation, the solution of (1.1) is approximated on a family of degree of freedom denoted by $\Sigma = \{\sigma_l\}_{l=1,\ldots,n_\Sigma}$. Typically, in each element K, we consider a family of points that are unisolvant for some interpolation spaces that are defined later in the text, typically subsets of $\mathbb{P}^k(K)$, the set of polynomials of degree $k \in \mathbb{N}$. The set Σ is the collection of these degrees of freedom. This enables us to define, from $\{u_i\}_{\sigma_i \in \Sigma}$, an interpolant u^h that we assume to be continuous. This is only possible under constraints on the degrees of freedom; examples are given in section 4.2. It is not necessary yet to go in more details. Last, for any σ_i, $\mathcal{V}_i$ denote the set of its neighbors.

We are interested in constructing high order convergent schemes for (1.1), that is, a functional $\mathcal{H}$ which is defined for any $\sigma \in \Sigma$, such that the approximation $u_j \simeq u(\sigma_j)$ of u at σ_j satisfies, for $i = 1, \ldots, n_\Sigma$,

$$\mathcal{H}(\sigma_i, u_i, \{u_j, j \in \mathcal{V}_i\}) = 0. \tag{1.6}$$

In (1.6), $\mathcal{V}_i$ is the set of neighbors of σ_i. This Hamiltonian has to be consistent in the meaning of Definition 1.1; this brings an implicit dependency with respect to the mesh and in particular, in h.

For technical reasons only, we need to extend the definition of the scheme to any point of Ω. This can be done as follows. We consider a subdivision of Ω of "control volumes" $\mathcal{C}_j$, $\Omega = \cup_{j=1}^{n_\Sigma} \mathcal{C}_j$ such that any control volume contains one and only one degree of freedom and conversely, any degree of freedom is contained in one and only

one control volume. After a convenient numbering, we can assume $\sigma_i \in \mathcal{C}_i$. We can also assume that a property similar to (1.5) also holds for this family of control volume. A possible construction of such control volume is given by a Voronoï diagram; see [2], for example. The functional $\mathcal{H}_h$ is extended on $\overline{\Omega}$ by the following: if $x \in \overline{\Omega}$, consider $\sigma \in \Sigma$ such that $x \in \mathcal{C}_\sigma$, and we set

$$\mathcal{H}\left(x, u^h(x), u^h\right) = \mathcal{H}(\sigma_i, u_i, \{u_j, j \in \mathcal{V}_i\}).$$

The approximation scheme (1.6) needs to be consistent with (1.1). We follow Barles and Souganidis' [3] definition.

DEFINITION 1.1 (consistant Hamiltonians). *We say that the Hamiltonian $\mathcal{H}$ is weakly consistent if for all $x \in \overline{\Omega}$ and $\phi \in C_b^\infty(\overline{\Omega})$ (the set of C^∞ bounded functions),*

$$\limsup_{h\to 0, y\to x, \xi\to 0} \mathcal{H}(y, \phi(y) + \xi, \phi + \xi) \le G^*(x, \phi(x), D\phi(x)) \tag{1.7}$$

and

$$\liminf_{\rho\to 0, y\to x, \xi\to 0} \mathcal{H}(y, \phi(y) + \xi, \phi + \xi) \ge G_*(x, \phi(x), D\phi(x)). \tag{1.8}$$

We say that $\mathcal{H}$ is strongly consistent if, whenever ϕ is linear (constant gradient), whatever $\sigma \in \Sigma$, $\sigma \in \Omega$,

$$\mathcal{H}(\sigma, \phi(\sigma), \phi) = H(\sigma, \phi(\sigma), D\phi(\sigma)).$$

Note that if $\mathcal{H}$ is weakly consistent, $\mathcal{H}$ is strongly consistent.

DEFINITION 1.2 (monotone Hamiltonians). *We say that $\mathcal{H}$ is monotone if, whenever $\sigma_i \in \Sigma$, $u_i \le v_j$ and for any $s \in \mathbb{R}$,*

$$\mathcal{H}(\sigma_i, s, \{u_j\}_{j\in\mathcal{V}_i}) \ge \mathcal{H}(\sigma_i, s, \{v_j\}_{j\in\mathcal{V}_i}).$$

There exists many numerical schemes devoted to the resolution of (1.1); examples are given by references [4, 5, 6, 7, 8], where the problem (1.1) is directly tackled.

One quite standard way of constructing a scheme for (1.1) is to consider the unsteady problem

$$\begin{aligned} &\frac{\partial v}{\partial t} + H(x, v(x), Du) = 0 \quad && x \in \Omega \subset \mathbb{R}^d, t > 0, \\ &v(x,t) = g(x,t) && x \in \partial\Omega, t > 0, \\ &v(x,0) = v_0(x) && x \in \Omega, t = 0 \end{aligned} \tag{1.9}$$

for some suitable initial condition u_0 such that the solution of (1.1) is obtained as the limit when $t \to +\infty$ of the solution of (1.9). There is a whole industry of numerical schemes for (1.9). Omitting the boundary conditions and in their simplest form, they are of the type

$$u_i^{n+1} = u_i^n - \Delta t \mathcal{H}(\sigma_i, u_i^n, \{u_j^n, j \in \mathcal{V}_i\}),$$

with $u_i^0 = u_0(\sigma_i)$. Along these lines, one may quote the work of [9, 6, 10] and among many others [11, 12] for Cartesian meshes and [13, 14, 15, 16] for unstructured meshes. To the best of our knowledge, the only convergence results, with error estimates, are for first order schemes; see [9, 17, 18] for structured meshes and [13] for unstructured

meshes. A general method for proving convergence, without error estimates, is given in [3]. All these constructions are strongly related to the different techniques that have been devised for constructing high order accurate, Godunov-type schemes for conservation laws.

Here, starting from a different construction, we explain how it is possible to construct *simple*, convergent, high order accurate schemes for the problem (1.1). We also show examples for which the computational stencil is the most possible compact. Our construction relies on the blending of a low order accurate scheme and a high order stable scheme. The structure of the blending parameter is analyzed so that high order accuracy is obtained as well as a convergence proof, however, without error estimate. These schemes are, of course, not monotone but monotonicity preserving. Up to our knowledge, it is the first time where both properties can simultaneously be achieved. We also study the practical implementation of the scheme and demonstrate its effectiveness on one-dimensional and two-dimensional examples. In this paper, we focus on unstructured triangular-type meshes. It is clear, however, that the main result of the paper (i.e., the form of the scheme and the convergence proof) can be used in a more general context.

The structure of this paper is the following: we first start by a general derivation of the scheme. We discuss in detail the structure of the blending parameter. We then provide a convergence proof. The next section is devoted to showing some examples of schemes, and we also discuss the practical implementation of the scheme. The last section is devoted to numerical examples.

2. Derivation of the schemes. We first discuss the scheme for the mesh points in the open set Ω. The boundary conditions are discussed at the end of this section.

We consider $\mathcal{H}_i^M := \mathcal{H}^M(\sigma_i, u_i, \{u_j\}_{j\in\mathcal{V}_i})$ a monotone consistent Hamiltonian and $\mathcal{H}_i^H := \mathcal{H}^H(\sigma_i, u_i, \{u_j\}_{j\in\mathcal{V}_i})$ a high order consistent Hamiltonian. By high order we mean that if u is a smooth solution of (1.1), then

$$\mathcal{H}^H(\sigma_i, u_i, \{u_j\}_{j\in\mathcal{V}_i}) = O\left(h^k\right) \tag{2.1}$$

for $k > 1$.

Next we consider for some $\ell \in \mathbb{R}$ the following Hamiltonian:

$$\mathcal{H}(\sigma_i, u_i, \{u_j\}_{j\in\mathcal{V}_i}) = \ell_i \mathcal{H}^M(\sigma_i, u_i, \{u_j\}_{j\in\mathcal{V}_i}) + (1-\ell_i)\mathcal{H}^H(\sigma_i, u_i, \{u_j\}_{j\in\mathcal{V}_i}) + \varepsilon(h). \tag{2.2}$$

We have the simple lemma, which proof is immediate.

LEMMA 2.1. *If $\mathcal{H}^M$ and $\mathcal{H}^H$ are strongly consistent, $\mathcal{H}$ defined by* (2.2) *is weakly consistent.*

We assume that $\varepsilon(h) = O(h^k)$. In order to define ℓ, we introduce the ratio $r_i := \frac{\mathcal{H}_i^H}{\mathcal{H}_i^M}$ and rewrite (2.2) as

$$\mathcal{H}(\sigma_i, u_i, \{u_j\}_{j\in\mathcal{V}_i}) = \left(\ell_i + (1-\ell_i)r_i\right)\mathcal{H}^M(\sigma_i, u_i\{u_j\}_{j\in\mathcal{V}_i}) + \varepsilon(h) \tag{2.3}$$

and choose ℓ such that

$$\ell_i + (1-\ell_i)r_i \geq \varepsilon'(h), \tag{2.4}$$

where $\varepsilon'(h)^{-1}\varepsilon(h) = o(1)$. The locus of the points (r, ℓ) that satisfy condition (2.4) lies between the two branches of the hyperbola $\ell + (1-\ell)r = 0$ displayed in Figure 2.1. Then, we can rewrite

$$|\mathcal{H}(x, t, \{u_j\}_{j\in\mathcal{V}_i})| \leq \left|\frac{\ell}{r} + 1 - \ell\right| \left|\mathcal{H}^M(x, t, \{u_j\}_{j\in\mathcal{V}_i})\right| + |\varepsilon(h)|\,. \tag{2.5}$$

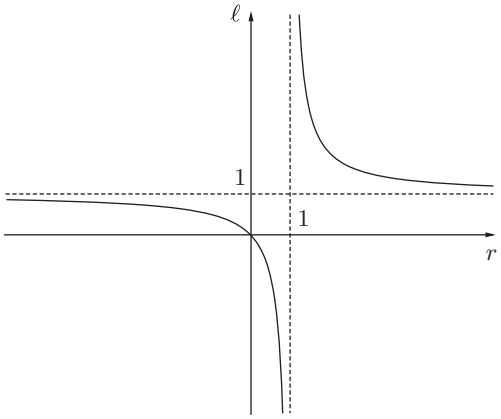

FIG. 2.1. *Graph of* $\ell + (1-\ell)r = 0$.

Since $\varepsilon(h) = O(h^k)$ and if $\ell \in [0,1]$, if there exists $C > 0$ such that

$$\left|\frac{\ell}{r}\right| \leq C, \tag{2.6}$$

then the scheme defined by the Hamiltonian (2.2) satisfies

$$\mathcal{H}(\sigma_i, u_i, \{u_j\}_{j\in\mathcal{V}_i}) = O\left(h^k\right)$$

for any smooth solution of (1.1).

Since the tangent at origin of the hyperbola $\{(r,\ell) \in \mathbb{R}^2, \ell + (1-\ell)r = 0\}$ is -1, a solution of the problem (2.6) is $\ell = \max(\ell^*, \varepsilon'(h))$, where

$$\ell^* = \begin{cases} 0 & \text{if } r \geq 0, \\ \min\left(1, \alpha|r|\right) & \text{else,} \end{cases} \tag{2.7}$$

for any $\alpha \geq 1$.

We have an additional constraint on ℓ. It comes from the iterative scheme that is needed to compute the solution of

$$\mathcal{H}(\sigma_i, u_i, \{u_j\}_{j\in\mathcal{V}_i}) = 0,$$

where $\mathcal{H}$ is defined by (2.2). In this paper, we employ the following explicit scheme:

$$\begin{aligned} u_i^{n+1} &= u_i^n - \Delta t \mathcal{H}\left(x_i, t, u_i^n, \{u_j^n\}_{j\in\mathcal{V}_i}\right) \quad \text{for } n \geq 1, \\ u_i^0 &= u_0(M_i). \end{aligned} \tag{2.8}$$

Up to our knowledge, all first order monotone Hamiltonians satisfy an L^∞ stability condition under a constraint on the time step of the type

$$\Delta t \leq Ch, \tag{2.9}$$

where C is a constant that depends only on u_0 and H, not on h the maximum diameter of the mesh elements. From (2.8), (2.3), and (2.4) we also have

$$u_i^{n+1} = u_i^n - \Delta t \left[(\ell_i + (1-\ell_i)r_i)\, \mathcal{H}^M(\sigma_i, u_i, \{u_j\}_{j\in\mathcal{V}_i}) + \varepsilon(h)\right]$$

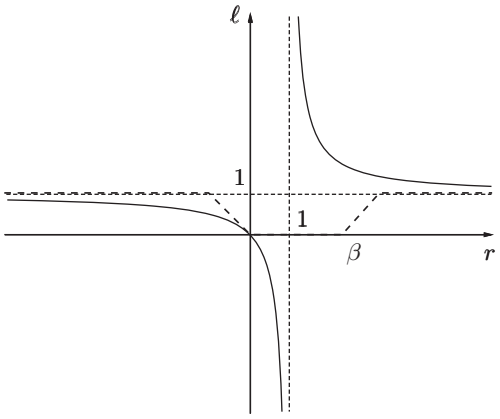

FIG. 2.2. *Graph of $\ell(r)$ corresponding to* (2.10).

so that the scheme is L^∞ stable if

$$\Delta t\,(\ell_i + (1-\ell_i)r_i) \le Ch.$$

In order to have Δt not too small, we consider $C' > 0$ and (r_i, ℓ_i) and $0 \le \ell_i \le 1$ such that

$$0 \le \ell_i + (1-\ell_i)r_i \le C'.$$

This imposes an additional condition only for $r_i > 0$. There are many ways of imposing this constraint in conjunction with (2.4). For simplicity reasons, given constants $\alpha_- \ge 1$, $\alpha_+ > 0$, and $\beta > 0$, we choose the following form for ℓ^*:

$$\ell^* = \begin{cases} \min(1, \alpha_- |r|) & \text{if } r \le 0, \\ 0 & \text{if } 0 \le r \le \beta, \\ \min(1, \alpha_+ (r-\beta)) & \text{else.} \end{cases} \tag{2.10}$$

The graph of such a function for $C = 1$ is displayed on Figure 2.2. With ℓ defined as in (2.10), there exists C' such that for

$$0 < \Delta t C' h, \tag{2.11}$$

the scheme defined by (2.8), (2.3), and (2.4) is L^∞ bounded.

Other choices are possible, such as

$$l^* = \varphi(r) := \frac{|r|}{1+|r|}$$

or, more generally,

$$l^* = \varphi(\psi(r)),$$

with $\psi(r) \ge r$ and $\psi'(0) = 1$. An example is $\psi(r) = r + r^2$. These possibilities have not been explored.

Since (1.1) does not depend on time, boundary conditions must be specified, otherwise the problem is meaningless. Here we follow the technique described in [19].

In order to simplify the text, we consider only first order accurate discretization of the boundary conditions.

We consider a boundary numerical Hamiltonian $\mathcal{H}_b$ that is consistent with a boundary Hamiltonian H_b. It is defined for $x \in \partial\Omega$, $s \in \mathbb{R}$, and $p \in \mathbb{R}^d$ and also satisfies

$$\forall x \in \partial\Omega, s \in \mathbb{R}, p \in \mathbb{R}^d, \qquad H_b(x,s,p) \le H(x,s,p).$$

The resulting scheme is as follows: find $\{u_j\}_{j=1,\dots,n_\Sigma}$ such that

(2.12a)
$$\text{if } \sigma_i \in \Omega, \qquad \ell_i \mathcal{H}^M\left(\sigma_i, u_i, \{u_j\}_{j\in\mathcal{V}_i}\right) + (1-\ell_i)\mathcal{H}^H\left(\sigma_i u_i, \{u_j\}_{j\in\mathcal{V}_i}\right) + \varepsilon(h) = 0,$$

(2.12b)
$$\text{if } \sigma_i \in \partial\Omega, \qquad \max\left(\mathcal{H}^b\left(\sigma_i, u_i, \{u_j\}_{j\in\mathcal{V}_i}\right), u_i - g(\sigma_i)\right) = 0.$$

The solution of (2.12) is not an easy task. Following standard techniques, we compute it as the limit when $n \to +\infty$, *if this limit exists*, of $\{u_j^n\}_{j=1,\dots,n_\Sigma}$, $n \in \mathbb{N}$ defined by $u_i^0 = u_0(x_i)$ and

(2.13a)
$$\text{if } \sigma_i \in \Omega, \qquad u_i^{n+1} = u_i^n - \Delta t\big(\ell_i \mathcal{H}^M\left(\sigma_i, u_i, \{u_j\}_{j\in\mathcal{V}_i}\right) + (1-\ell_i)\mathcal{H}^H\left(\sigma_i u_i, \{u_j\}_{j\in\mathcal{V}_i}\right) + \varepsilon(h)\big),$$

(2.13b)
$$\text{if } \sigma_i \in \partial\Omega, \qquad \max\left(\frac{u_i^{n+1}-u_i^n}{\Delta t} + \mathcal{H}^b\left(\sigma_i, u_i, \{u_j\}_{j\in\mathcal{V}_i}\right), u_i^{n+1} - g(x_i)\right) = 0.$$

In (2.12) and (2.13), ℓ is defined by (2.10).

In the following, we extend the definition of ℓ to any $x \in \Omega$ as we have done for the Hamiltonian via the explicit dependency of the ratio r in x.

3. Convergence proof. We denote by S the operator

$$S(h,x,u_h) = \begin{cases} \ell(x)\mathcal{H}^M\left(x, u_h(x), u_h\right) + (1-\ell(x))\mathcal{H}^H\left(x, u_h(x), u_h\right) + \varepsilon(h) & \text{if } x \in \Omega, \\ \max\left(\mathcal{H}^b\left(x, u_h(x), u_h\right), u_h(x) - g(x)\right) = 0 \text{ if } x \in \partial\Omega. \end{cases}$$

We have the following result.

THEOREM 3.1. *We consider the scheme* (2.12) *and assume that*

1. $\mathcal{H}^M$, $\mathcal{H}^H$, *and* $\mathcal{H}_b$ *are strongly consistent;*
2. $\mathcal{H}^M$ *and* $\mathcal{H}_b$ *are monotone Hamiltonians;*
3. $H_b \le H$*;*
4. *the blending parameter* ℓ *belongs to* $[0,1]$ *and satisfies*

$$r = \frac{\mathcal{H}^H(x, u_h(x), u_h)}{\mathcal{H}^M(x, u_h(x), u_h)}, \qquad \ell(x) + (1-\ell(x))r \ge \varepsilon'(h),$$

   where the parameters $\varepsilon(h)$ *and* $\varepsilon'(h)$ *satisfy* $\varepsilon'(h)^{-1}\varepsilon(h) = o(1)$*;*
5. *there exists a unique solution of* (2.12) u_h *that satisfies* L^∞ *bound that is uniform in* h*;*
6. *Equation* (1.1) *has a uniqueness principle.*

Then the family u_h *defined by* (2.12) *converges locally uniformly to the solution of* (1.1) *in* Ω*.*

Remark 1. An essential ingredient in Theorem 3.1 is that the scheme (2.12) has a unique solution which is bounded in L^∞ uniformly in h. In practical calculations,

the solution is obtained by an iterative scheme: we look for the limit, when $n \to +\infty$, of the iterative scheme (2.13) (for example, (2.13)), *if such limit exists.* If such a limit exists, the L^∞ bound comes from the CFL condition (2.11), but the existence of the limit is not a trivial statement.

Proof of Theorem 3.1. We proceed as in [1]. The sequence u_h is bounded, so we can define

$$\overline{u}(x) = \limsup_{y\to x, h\to 0} u_h(y) \text{ and } \underline{u}(x) = \liminf_{y\to x, h\to 0} u_h(y).$$

They are defined on $\overline{\Omega}$ because u_h has bounds independent of h. We show that the functions $\overline{u}$ and $\underline{u}$ are, respectively, subsolutions and supersolutions of (1.1). We proceed in two parts: first, we consider the case of an interior point, then the case of a boundary point.

Case of an interior point. In fact, we show first that if $x_0 \in \Omega$ is a local maximum of $\overline{u} - \phi$ for some $\phi \in C^b_\infty(\Omega)$, then

$$H(x_0, \varphi(x_0) D\varphi(x_0)) \le 0, \tag{3.1}$$

while if $x_0 \in \Omega$ is a local minimum of $\underline{u} - \phi$,

$$H(x_0, \varphi(x_0) D\varphi(x_0)) \ge 0. \tag{3.2}$$

To show the inequality (3.2), we repeat Barles and Souganidis' arguments; the inequality (3.2) is obtained in the same way. We may assume that x_0 is a strict minimum $\underline{u}(x_0) = \phi(x_0)$, $\phi \le 2 \inf_h ||u_h||_\infty$ outside of $B(x_0, r)$, where r is such that

$$\underline{u}(x) - \phi(x) \ge \underline{u}(x_0) - \phi(x_0) = 0 \text{ in } B(x_0, r).$$

There exists sequences h_n and $y_n \in \overline{\Omega}$ such that $n \to +\infty$, $h_n \to 0$, $y_n \to x_0$, $u_{h_n}(y_n) \to \underline{u}(x_0)$, and y_n is a global minimum of $u_{h_n} - \phi$. We denote by ξ_n the quantity $u_{h_n}(y_n) - \phi(y_n)$. We have $\xi_n \to 0$, $u_{h_n}(y) \ge \phi(y) + \xi_n$ in $B(x_0, r)$.

Defining $r_n = \frac{\mathcal{H}^H_{h_n}(y_n, u_h(y_n), u_h)}{\mathcal{H}^M_{h_n}(y_n, u_h(y_n), u_h)}$, we get

$$\begin{aligned} 0 &= \ell(y_n)\mathcal{H}^M_{h_n}(y_n, u_h(y_n), u_h) + (1-\ell(y_n))\mathcal{H}^H(y_n, u_h(y_n), u_h) + \varepsilon(h_n) \\ &= (\ell(y_n) + (1-\ell(y_n))r_n)\,\mathcal{H}^M(y_n, u_h(y_n), u_h) + \varepsilon(h_n). \end{aligned} \tag{3.3}$$

Since

$$0 \le \frac{\varepsilon(h_n)}{\ell(y_n) + (1-\ell(y_n))r_n} \le \frac{\varepsilon(h_n)}{\varepsilon'(h_n)} = o(1),$$

we have since $\ell(y_n) + (1-\ell(y_n))r \ge \varepsilon'(h) > 0$, we get all in all

$$\frac{\varepsilon(h_n)}{\ell(y_n) + (1-\ell(y_n))r_n} = o(1),$$

because $\mathcal{H}^M$ is monotone and $\varepsilon'(h) > 0$. Hence, if we divide the last equality of (3.3) by $\ell(y_n) + (1-\ell(y_n))r_n > \varepsilon'(h_n) > 0$, we get

$$0 \le \mathcal{H}^M_{h_n}(y_n, u_h(y_n), u_h) + o(1). \tag{3.4}$$

Last, using the monotonicity of $\mathcal{H}^M_{h_n}$, we end up to

$$0 \le \mathcal{H}^M_{h_n}(y_n, \phi(y_n) + \xi_n, \phi + \xi_n) + o(1). \tag{3.5}$$

Note that in passing from (3.4) to (3.5), we have used the uniform continuity of H.

Thus

$$\begin{aligned} 0 &\le \limsup_n \mathcal{H}^M(y_n, \phi(y_n) + \xi_n, \phi + \xi_n) \\ &\le H(x_0, \varphi(x_0), D\varphi(x_0)). \end{aligned}$$

This shows that $\underline{u}$ is a supersolution of (1.1). The same arguments applied to $\overline{u}$ show that it is a subsolution of (1.1) in Ω.

Case of a boundary point. Now we consider the case of $x_0 \in \partial\Omega$. The first remark is that for $x \in \partial\Omega$ and any $\varphi \in C^\infty_b(\overline{\Omega})$,

$$\begin{aligned} \limsup_{h\to 0, y\to x, \xi\to 0} S(h, x, \varphi + \xi) &= \max(H(x,\varphi(x), D\varphi), \\ &\qquad \max(H_b(x, \varphi(x), D\varphi(x)), \varphi(x) - g(x))), \\ \liminf_{h\to 0, y\to x, \xi\to 0} S(h, x, \varphi + \xi) &= \min(H(x,\varphi(x), D\varphi), \\ &\qquad \max(H_b(x, \varphi(x), D\varphi(x)), \varphi(x) - g(x))). \end{aligned}$$

The proof for showing that if $x_0 \in \partial\Omega$ is a local maximum of $\overline{u} - \phi$ for some $\phi \in C^b_\infty(\overline{\Omega})$, then

$$\min(H(x_0, \varphi(x_0) D\varphi(x_0)), \max(H_b(x_0, \varphi(x_0), D\varphi(x_0)), \varphi(x_0) - g(x_0))) \le 0, \tag{3.6}$$

while if $x_0 \in \overline{\Omega}$ is a local minimum of $\underline{u} - \phi$,

$$\max(H(x_0, \varphi(x_0) D\varphi(x_0)), \max(H_b(x_0, \varphi(x_0), D\varphi(x_0)), \varphi(x_0) - g(x_0))) \ge 0 \tag{3.7}$$

can easily be obtained by combining the same arguments and those of [19, Theorem 2.2].

Since S is monotone, we get

$$\begin{aligned} 0 \le \limsup_n S(h_n, y_n, \phi(y_n) + \xi_n) &\le \limsup_{h\to 0, y\to x, \xi\to 0} S(h, y, \varphi + \xi) \\ &= \max(H(x_0, \varphi(x_0), D\varphi(x_0)), \\ &\qquad \max(H_b(x_0, \varphi(x_0), D\varphi(x_0)), \\ &\qquad F(x, \varphi(x_0), D\varphi(x_0)))). \end{aligned}$$

Now we have to check that the condition (3.6) (resp. (3.7)) implies the supersolution (resp. subsolution) condition.

- **Inequality (3.6).** If $F(x_0, \underline{u}(x_0), D\phi(x_0)) \le 0$, there is nothing to prove. We assume $F(x_0, \underline{u}(x_0), D\phi(x_0)) > 0$. We have either

  $$H(x_0, \varphi(x_0), D\varphi(x_0)) \le 0 \tag{3.8}$$

  or

  $$\max(H_b(x_0, \underline{u}(x_0), D\phi(x_0)), F(x_0, \underline{u}(x_0), D\phi(x_0)) \le 0.$$

  In the second case, we have necessarily (3.8) and in both cases, the inequality holds.

- **Inequality (3.7).** If $F(x_0, \underline{u}(x_0), D\phi(x_0)) \geq 0$, there is nothing to prove. Assume $F(x_0, \underline{u}(x_0), D\phi(x_0)) < 0$, then we must have either $H(x_0, \underline{u}(x_0), D\phi(x_0)) \geq 0$ or

$$\max(H_b(x_0, \underline{u}(x_0), D\phi(x_0)), F(x_0, \underline{u}(x_0), D\phi(x_0))) \geq 0.$$

Since $F < 0$, this inequality implies $H_b \geq 0$ so that

$$H(x_0, \underline{u}(x_0), D\phi(x_0)) \geq H_b(x_0, \underline{u}(x_0), D\phi(x_0)) \geq 0.$$

Thus, in both cases, we get $H(x_0, \underline{u}(x_0), D\phi(x_0)) \geq 0$, which is what we wanted.

Conclusion. All this shows that $\underline{u}$ is a supersolution and $\overline{u}$ is a subsolution of (1.1). The strong uniqueness principle enables us to conclude. ∎

Remark 2.

1. *Choice of $\varepsilon(h)$ and $\varepsilon'(h)$.* Since we must have $\varepsilon(h) = O(h^k)$, $\ell = O(h^k)$, and $\varepsilon'(h)^{-1}\varepsilon(h) = o(1)$, a good choice for $\varepsilon(h)$ and $\varepsilon'(h)$ is $\varepsilon(h) = Ch^{k+1}$ and $\varepsilon(h) = C'h^k$ for any constants C, C'.
   In the numerical applications, however, we have chosen $\varepsilon'(h) = 0$; that seems to work fine.
2. *Consistency of $\mathcal{H}^H$.* The proof does not make any use of the consistency of $\mathcal{H}^H$. Only $\mathcal{H}^M$ matters. However, since $\mathcal{H}^H$ satisfies (2.1), it must be consistent.

4. Examples of schemes and practical implementation.

4.1. First order numerical schemes. We consider two kinds of first order schemes: the Godunov scheme and the Lax–Friedrichs scheme. We recall briefly their construction here. We describe their construction for elements, and the degrees of freedom are the vertices of these elements. To make the text simpler, we implicitly assume that the elements are triangles in two dimensions (2D), but this is absolutely not essential.

Godunov Hamiltonian. If $H = H_1 + H_2$, where H_1 (resp. H_2) is convex (resp. concave), then we set

$$\mathcal{H}_h^G(p_1, \ldots, p_{k_i}) = \inf_{q \in \mathbb{R}^2} \max_{0 \leq l \leq k_i} \sup_{y \in -\Omega_l + q} \left[p_i \cdot (y - q) - H_1^*(y) - H_2^*(q) \right], \tag{4.1}$$

where Ω_l, $l = 1, \ldots, k_1$ are the angular sectors defined by the triangles $T_1, \ldots, T_{k_i}$ at node M_i, H_1^*, and H_2^* are the Legendre transforms of H_1 and H_2. We have denoted by $x \cdot y$ the dot product of x and y.

If h is the smallest radius of the circles of center M_i contained in $\cup_{i=1}^{k_i} T_j$, if L_1 and L_2 are Lipschitz constants for H_1 and H_2, then the scheme is monotone provided that the time step satisfies

$$\frac{\Delta t}{h}(L_1 + L_2) \leq \frac{1}{2};$$

one can consult [13] for more details.

In most of the numerical examples below, the Hamiltonian is convex, so (4.1) becomes simpler:

$$\mathcal{H}_h^G(p_1, \ldots, p_{k_i}) = \max_{0 \leq l \leq k_i} \sup_{y \in -\Omega_l} \left[p_i \cdot y - H_1^*(y) \right]. \tag{4.2}$$

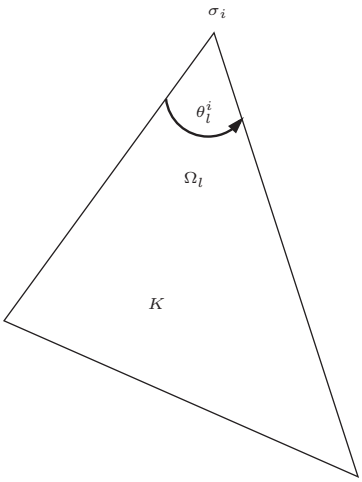

FIG. 4.1. *The angular sector in the element K at σ_i.*

We denote by H_T the term $\sup_{y\in-\Omega_l}[p_i\cdot y - H_1^*(y)]$, where the angular sector Ω_l is the sector of T seen from the vertex M.

Remark 3. The implementation of this Hamiltonian is very easy if the evaluation of

$$\sup_{y\in-\Omega_l}[p_i\cdot y - H_1^*(y)]$$

is simple. We first need to initialize $\mathcal{H}_i^G := \mathcal{H}^G(\sigma_i, u_i^h, u_h)$ to a large negative value. We then make a loop over the elements of the mesh, evaluate for each element the gradient of the piecewise linear interpolant u_h, evaluate for each vertex of the element the quantity

$$\mathcal{H}_i^T := \sup_{y\in-\Omega_l}[p_i\ \cdot\ y - H_1^*(y)]\,,$$

where, for the vertex σ_i, Ω_l is the sector of the element as in Figure 4.1.

Lax–Friedrichs Hamiltonian. Here we set

$$\mathcal{H}_h^{LF}(Du_{\Omega_1},\dots,Du_{\Omega_{k_i}}) = H\left(\bar{U}\right) - \frac{\epsilon}{h}\oint_{C_h}[u(M)-u(M_i)]dl, \tag{4.3a}$$

where C_h (resp. D_h) is a circle (disk) of center M_i and radius h,

$$\widehat{U} = \frac{\int_{D_h} Du\ dxdy}{\pi h^2},$$

and ϵ is larger than any Lipschitz constant of H divided by 2π.

A different version of the Lax–Friedrichs Hamiltonian that is monotone under the same constraint is the following:

$$\mathcal{H}_h^{LF}(Du_{\Omega_1},\dots,Du_{\Omega_{k_i}}) = \frac{\displaystyle\int_{D_h} H(Du)}{\pi h^2} - \frac{\epsilon}{h}\oint_{C_h}[u(M)-u(M_i)]dl. \tag{4.3b}$$

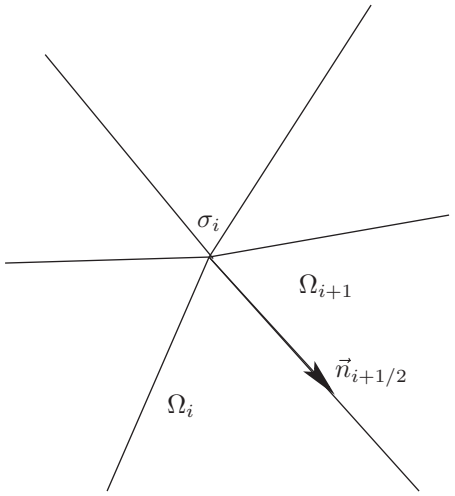

FIG. 4.2. *Illustration of the angular sectors Ω_i and the vectors $\vec{n}_{i+1/2}$ that are needed in* (4.3a).

This version can be rewritten as

$$\mathcal{H}_h^{LF}(Du_{\Omega_1},\dots,Du_{\Omega_{k_i}}) = \sum_{0\le l\le k_i} \frac{\theta_l^i}{2\pi} H\left(Du_{\Omega_l^i}\right) + \varepsilon \sum_{0\le l\le k_i} \tan\theta_l^i \frac{\vec{n}_{l-1/2}^i + \vec{n}_{l+1/2}^i}{2}\cdot Du_{\Omega_l^i}.$$

The vector $\vec{n}_{l+1/2}$ is the unit vector of the edge that separates the angular sectors Ω_l and Ω_{l+1}, the angle θ_l^i is the angle of the angular sector at σ_i; see Figure 4.2. The parameter ε is the same as in the previous version.

A third version, which is the one we have used in the simulations, is

$$\mathcal{H}^{LF}\left(Du_{\Omega_1},\dots,Du_{\Omega_{k_i}}\right) = \frac{\displaystyle\sum_{T\ni M_i} |T| H(Du_{|T}) + \alpha \sum_{M_j\in T} (u_i - u_j)}{\displaystyle\sum_{T\ni M_i} |T|} \tag{4.3c}$$

and $\alpha \ge h_T \max_p ||D_p H||$, where h_T is the largest edge of T.

The main difference between these different formulas is that (4.3a) and (4.3b) are intrinsic in the sense given in [13], while (4.3c) is not. By the way, the same is true for (4.1). Hence, following the same reference, (4.3a) and (4.3b) are convergent, and the error estimate is $\mathcal{O}(h^{1/2})$. For (4.3c), such an error estimate is not available (at least when following the technique of [13]), but it is convergent: this is a simple application of [3].

The advantage of (4.3c) over the other two versions is its simplicity in coding. As (4.3b), we need to make a loop over the element. For each element, we compute $Du_{|T}$, α and evaluate for each degree of freedom in the element

$$|T| H(Du_{|T}) + \alpha(u_i - u_j).$$

The numerical Hamiltonian is the arithmetic average of these quantities.

The dissipation mechanisms are much simpler than for (4.3b). Considering (4.3a), the loop has to be carried out over each degree of freedom. Then for each of them, we need to make a loop over its neighbors. In the case of (4.3c), the coding is *much* simpler; this is why we prefer (4.3c).

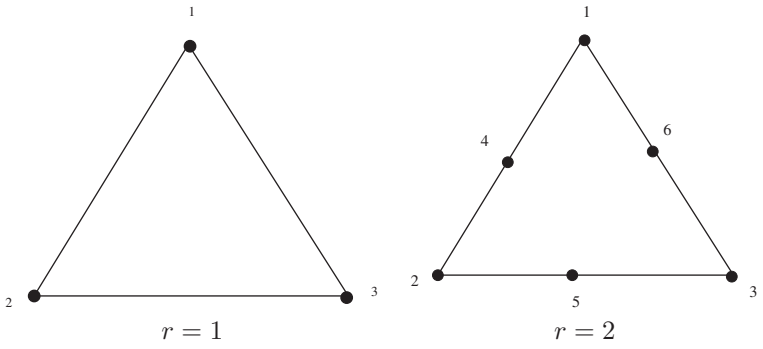

FIG. 4.3. *Degrees of freedom for* $r = 1$, $r = 2$.

4.2. High order Hamiltonians. There are many formally high order numerical Hamiltonians, but it is more difficult to construct stable and high order Hamiltonians. For example, if a discrete L^2-like stability property is sought, one has to realize that there is no natural counterpart on the continuous side because of the nature of the viscosity solutions: the test functions are not integrated by part as for standard hyperbolic problems. The natural L^2-like stability property has to be written on Du. This causes some difficulties that may be overcome; see, for example, [14] and more recently [20]. In the following, we first consider a formally high order scheme that appears to be stable as long as no singularity of Du appear. It is in the spirit of the ENO-like scheme of [6, 21] and [13]. A second example is also considered following [15]. The scheme is more compact but adapted only to homogeneous Hamiltonians. However, we propose an ad hoc extension to the inhomogeneous case in this paper.

Notations. In this paragraph, we consider elements that are implicitly thought as triangular elements, but this restriction is not essential. We first precise the type of interpolant (reconstruction) of $\{u_i\}_{i=1,\dots,n_\Sigma}$ we consider in the examples.

Two kinds of Lagrange-type interpolants are considered. Since there is no ambiguity when we consider a given interpolation, u^h represents the interpolation of the continuous function u.

In the first case, in each triangle T, the solution is approximated by a polynomial of degree r; their set is $\mathbb{P}^k(T)$. Hence, the solution is described by $\frac{(r+1)(r+2)}{2}$ degrees of freedom. It is known that the points of T which barycentric coordinates are $(\frac{i}{r}, \frac{j}{r}, \frac{k}{r})$, with i, j, k positive integers, and $i + j + k = r$ are unisolvant. Examples for $r = 1$, 2 are displayed on Figure 4.3. The degrees of freedom σ in the mesh is the collection of these new points.

Other choices are possible, such as the interpolants defined in [22]. The simplest example is described, in any triangle, by the degrees of freedom consisting of those of the $\mathbb{P}^2$ interpolation plus the centroid of the triangle; see Figure 4.4. Denoting by vec(b) the set of functions of the type λb where $\lambda \in \mathbb{R}$, the interpolation space is $\widetilde{\mathbb{P}}^2(T) = \mathbb{P}^2(T) \bigoplus \text{vect}(b)$. The bubble function is, if $\{\Lambda_j\}_{j=1,3}$ denotes the barycentric coordinates in T, $b = \Lambda_1\Lambda_2\Lambda_3$. This interpolation space is used in the two-dimensional examples. It yields a third order accurate interpolation and enjoys the following quadrature relation:

$$\int_T f(x)dx = |T| \sum_j \omega_j f(x_j), \tag{4.4}$$

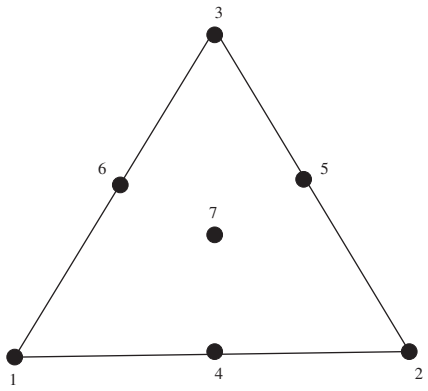

FIG. 4.4. *Location of the degrees of freedom for the third order accurate example of* [22].

with $\omega_j = \frac{1}{20}$ for $j = 1, \ldots, 3$, $\omega_j = \frac{2}{15}$ for $j = 4, \ldots, 6$, and $\omega_7 = \frac{9}{20}$. See [22] for more details and other examples.

We describe the basis functions for $\mathbb{P}^1(T)$, $\mathbb{P}^2(T)$, and $\widetilde{\mathbb{P}}^2(T)$. We follow the notations of Figures 4.3 and 4.4.

- *Case* $\mathbb{P}^1(T)$. We have $\mathcal{N}_i = \Lambda_i$.
- *Case* $\mathbb{P}^2(T)$. We have $\mathcal{N}_1 = \Lambda_1(2\Lambda_1 - 1)$ and similar formula for $i = 2, 3$; $\mathcal{N}_4 = 4\Lambda_1\Lambda_4$ and similar formula for $i = 5, 6$.
- *Case of* $\widetilde{\mathbb{P}}^2(T)$. The basis functions are $\mathcal{N}_1 = \Lambda_1(2\Lambda_1) + 3b$ and similar formula for $i = 2, 3$; $\mathcal{N}_4 = 4\Lambda_1\Lambda_3 - 12b$ and similar formula for $i = 5, 6$; $\mathcal{N}_7 = 27b$.

The main difference between the basis functions of $\mathbb{P}^2(T)$ and those of $\widetilde{\mathbb{P}}^2(T)$ is that $\int_T \mathcal{N}_\sigma dx = 0$ for $\sigma = 1, 2, 3$ in $\mathbb{P}^2(T)$, while $\int_T \mathcal{N}_\sigma dx > 0$ for any σ in $\widetilde{\mathbb{P}}^2(T)$. This behavior plays an important role in the next paragraph.

Other types of Lagrange interpolants could have been considered.

4.2.1. ENO/WENO-like schemes. Consider any degree of freedom σ. It belongs to several triangles T, possibly only one if $r \geq 3$. Denote by $\mathcal{V}_\sigma$ the list of these triangles. We define the high order Hamiltonian as

$$\mathcal{H}_\sigma^H := \mathcal{H}^M \left(Du_{T_k}^h, T_k \in \mathcal{V}_\sigma \right), \tag{4.5}$$

where $\mathcal{H}^M$ is any of the low order Hamiltonians defined above by (4.1), (4.2), (4.3a), or (4.3b). Other high order Hamiltonians, such as the high order central one of [23, 16] could have been considered.

In the very early draft of this work, (4.5) has been implemented and tested. We do not present the results here, mainly because we want to stress the simplicity aspect of our derivation. In the case of ENO/WENO-type scheme, the reconstruction step is very complex, especially for unstructured meshes. In the next section, we present a much simpler method for constructing high order scheme, which has led us to abandon the ENO one.

4.2.2. Compact schemes numerical Hamiltonians. In this section, for any triangle, the interpolant u^h belongs to $\mathbb{P}^1(T)$ or $\widetilde{\mathbb{P}^2(T)}$.

Derivation. We follow [15]: in the case of a homogeneous Hamiltonian of degree k in $\mathbf{p}$, for example,

$$H(x, u, \mathbf{p}) \equiv H(\mathbf{p}) - f(x),$$

with

$$H(\mathbf{p}) = \frac{1}{k} D_{\mathbf{p}} H(\mathbf{p}) \cdot \mathbf{p},$$

we can look at

$$H(x, Du) = 0$$

as a convection problem with source term

$$\vec{\lambda} \cdot Du = f(x), \tag{4.6}$$

where $\vec{\lambda} = \frac{1}{k} D_{\mathbf{p}} H(Du)$.

Then we consider the unsteady problem associated to this equation (without the boundary conditions)

$$\frac{\partial u}{\partial t} + \frac{1}{p} H_p(Du) \cdot Du = f(x),$$

i.e., a convection-like problem which is approximated, via the streamline upwind Petrov–Galerkin (SUPG) method [24], as

$$\begin{aligned} &\int_{\Omega \times [t_n, t_{n+1}]} \omega \left(\frac{\partial u}{\partial t} + H(x, Du) \right) dx \\ &\quad + \int_{\Omega \times [t_n, t_{n+1}]} \left(\frac{\partial \omega}{\partial t} + DH \cdot D\omega \right) \tau \left(\frac{\partial u}{\partial t} + H(x, Du) \right) = 0, \end{aligned} \tag{4.7}$$

where ω is any linear combination of the basis functions $\mathcal{N}_\sigma(x)\varphi(t)$, with φ linear in time. The positive real number τ is typically chosen as

$$\tau = \left(\left(\frac{2}{\Delta t} \right)^2 + \left(\frac{2|D_p H|}{h} \right)^2 \right)^{-1/2}.$$

Noticing that

$$\frac{\partial \omega}{\partial t} = \frac{\omega(x, t_{n+1}) - \omega(x, t_n)}{\Delta t},$$

using (4.4) we apply mass lumping and get

$$\frac{u_\sigma^{n+1} - u_\sigma^n}{\Delta t} + \mathcal{H}_\sigma \left(\sigma, u_\sigma, u_{\xi_{\xi \in \mathcal{V}_\sigma}} \right) = 0,$$

with

$$\begin{aligned} &\mathcal{H}_\sigma \left(\sigma, u_\sigma, u_{\xi_{\xi \in \mathcal{V}_\sigma}} \right) \\ &:= \left(\int_\Omega H\left(\sigma, Du^h\right) \mathcal{N}_\sigma dx \right. \\ &\quad \left. + h \int_\Omega \left[\frac{D_{\mathbf{p}} H\left(\sigma, Du^h\right)}{\| D_{\mathbf{p}} H\left(\sigma, Du^h\right) \|} \cdot D\mathcal{N}_\sigma \right] H\left(\sigma, Du^h\right) dx \right) \left(\int_\Omega \mathcal{N}_\sigma dx \right)^{-1}. \end{aligned} \tag{4.8}$$

In (4.8), h is the maximum diameter of the triangle of the mesh. The Hamiltonian (4.8) will be used for (1.1) when H is homogeneous in $p = Du$. Modifications for the inhomogeneous case are considered later.

We have the simple lemma, which can easily be generalized to other types of interpolants.

LEMMA 4.1. *Assume H is C^1 and consider the interpolant in $\mathbb{P}^1(T)$ or $\widetilde{\mathbb{P}^2(T)}$ where linear functions are preserved. Away from the boundaries, relation* (4.8) *defines a consistent Hamiltonian in the meaning given by Definition* 1.1.

Proof. If u is linear, $u^h = u$. For any degree of freedom σ, we have

$$\left(\int_\Omega H\left(\sigma, Du^h\right)\mathcal{N}_\sigma dx\right)\left(\int_\Omega \mathcal{N}_\sigma dx\right)^{-1} = H(\sigma, Du(\sigma)) \tag{4.9a}$$

because Du is constant.

Since σ is not on the boundary of Ω, the support of $\mathcal{N}_\sigma$ lies inside of Ω, and thus

$$\int_\Omega D\mathcal{N}_\sigma dx = 0.$$

The second term in (4.8) gives

$$\begin{aligned}\int_\Omega \left[\frac{D_{\mathbf{p}}H\left(\sigma, Du^h\right)}{\|D_{\mathbf{p}}H\left(\sigma, Du^h\right)\|}\cdot D\mathcal{N}_\sigma\right] H\left(\sigma, Du^h\right) dx \\ = H(\sigma, Du)\left[\frac{D_{\mathbf{p}}H\left(\sigma, Du^h\right)}{\|D_{\mathbf{p}}H\left(\sigma, Du^h\right)\|}\right]\cdot\int_\Omega D\mathcal{N}_\sigma dx \\ = 0.\end{aligned} \tag{4.9b}$$

Using (4.9a) and (4.9b) and Definition 1.1, the Hamiltonian (4.8) is consistent. ∎

Remark 4.

1. The choice of the basis functions is fundamental because $\int_\Omega \mathcal{N}_\sigma dx$ needs to be nonzero.
2. The proof does not depend on the fact that the Hamiltonian is homogeneous. It can be easily adapted to the case where the "dissipation" parameter $\frac{D_{\mathbf{p}}H(x,Du^h)}{\|D_{\mathbf{p}}H(x,Du^h)\|}$ is replaced by $\mathcal{D}H$, a continuous vector-valued function.

We first review the stability properties of (4.8) for homogeneous Hamiltonians from [15].

Stability property. As mentioned several times earlier in the text, the Hamiltonian (4.8) must satisfy some stability property. Here, we recall some results of [15] where they show that this is, indeed, the case, at least when a particular integration scheme of (4.7) is chosen.

In [15], the Hamiltonian (4.8), introduced for Hamiltonians that are homogeneous of degree k in the Du variable, have the property that (4.8) and (4.7) satisfy a minimization principle for $f = 0$. Their remark is trivially extended to $f \not\equiv 0$. This ensures a stability condition. For example, the following inequality is shown in [15]:

Setting $t_n = n\Delta t$, we have

(4.10)
$$\frac{1}{2}\left\|u\left(t_-^N\right)\right\|_\Omega^2+\frac{1}{2}\sum_{n=0}^{N-1}\left\|u\left(t_+^n\right)-u\left(t_-^n\right)\right\|_\Omega^2+\sum_{n=0}^{N-1}\left\|\sqrt{\tau}\left(\frac{\partial u}{\partial t}+H(x,u,Du)\right)\right\|^2_{\Omega\times[t_n,t_{n+1}]}$$
$$+\frac{1}{2}\sum_{n=0}^{N-1}\sum_{T\in\mathcal{T}}\int_{t_n}^{t_{n+1}}\int_T u^2\left(D\cdot DH\right)dxdt$$
$$=\frac{1}{2}\left\|u\left(t_-^0\right)\right\|_\Omega^2.$$

This relation shows that the (implicit in time) Petrov–Galerkin scheme (4.7) is energy stable.

Accuracy arguments. We show now that the scheme (4.8) is high order accurate for the *steady* problem (1.1) in which we omit the boundary conditions. We assume that the solution u is smooth enough so that this formal calculation is, indeed, valid. We have, strongly, that for any x, $H(x,u(x),Du(x))=0$. So, if I^hu denotes the interpolant of the exact solution, we see that the truncation error in terms of the gradient of the error $e^h=u^h-I^hu$ satisfies

$$\int_\Omega\left[H\left(x,u^h,Du^h\right)-H\left(x,I^hu,DI^hu\right)\right]\mathcal{N}_\sigma$$
$$+\ h\int_\Omega\left[\frac{H_p(Du^h)}{||H_p(Du^h)||}\cdot D\mathcal{N}_\sigma\right]\left[H\left(x,u^h,Du^h\right)-H\left(x,I^hu,DI^hu\right)\right]dx$$
$$=\mathcal{O}\left(h^k\right)\times\left[\int_\Omega\mathcal{N}_\sigma\right]dx$$

if $u-I^hu=\mathcal{O}(h^k)$ in a suitable norm, $k=2$ for $\mathbb{P}^1(T)$, and $k=3$ for $\widetilde{\mathbb{P}^2(T)}$. This relation indicates that $H(x,u^h,Du^h)-H(x,I^hu,DI^hu)=\mathcal{O}(h^k)$ in the same norm, so that $De^h=\mathcal{O}(h^k)$. This is clearly not a proof, only an indication of the formal accuracy of the scheme. We see that we get an extra order, thanks to the fact that the exact solution u satisfies, for any σ, the residual property

$$\int_\Omega H(x,u,Du)\mathcal{N}_\sigma dx+h\int_\Omega\left[\frac{D_{\mathbf{p}}H\left(x,u^h,Du^h\right)}{\|D_{\mathbf{p}}H\left(x,u^h,Du^h\right)\|}\cdot D\mathcal{N}_\sigma\right]\ H(x,u,Du)dx=0.$$

Case of inhomogeneous Hamiltonians. The difficult problem is to control the term

$$\left(h\int_\Omega\left[\frac{D_{\mathbf{p}}H\left(x,Du^h\right)}{\|D_{\mathbf{p}}H\left(x,Du^h\right)\|}\cdot D\mathcal{N}_\sigma\right]\ H\left(x,Du^h\right)dx\right)\left(\int_\Omega\mathcal{N}_\sigma dx\right)^{-1} \tag{4.11}$$

of (4.8). For a homogeneous Hamiltonian of the type $H(x,u,\mathbf{p})\equiv H(\mathbf{p})-f(x)$, with H homogeneous of degree >0, this term clearly brings dissipation because

$$D_{\mathbf{p}}H\left(x,Du^h\right)\cdot D\mathcal{N}_\sigma\ \ H\left(x,Du^h\right)=\frac{1}{p}\left(D_{\mathbf{p}}H\left(x,Du^h\right)\cdot D\mathcal{N}_\sigma\right)\ \left(D_{\mathbf{p}}H\left(x,Du^h\right)\cdot Du^h\right)$$
$$-D_{\mathbf{p}}H\left(x,Du^h\right)\cdot D\mathcal{N}_\sigma\ \ f(x).$$

The second term plays the role of a source term and does not affect the stability.

In the inhomogeneous case, this argument does not work any longer, but if we write

$$H\left(x,u,Du^h\right)=\mathcal{DH}\left(x,u^h\right)\cdot\left(Du^h-p^{\text{ref}}\right)+H\left(x,u,p^{\text{ref}}\right),$$

where p^{ref} is any reference vector, if the mapping $Du^h\mapsto\mathcal{DH}(x,u^h)$ is continuous (so that the numerical Hamiltonian remains consistent), we can repeat formally the stability argument by replacing (4.11) in (4.8) by

$$h\frac{\displaystyle\int_\Omega\left[\frac{\mathcal{DH}\left(x,u^h\right)}{\|\mathcal{DH}\left(x,u^h\right)\|}\cdot D\mathcal{N}_\sigma\right]\,H\left(x,u^h,Du^h\right)dx}{\displaystyle\int_\Omega\mathcal{N}_\sigma dx}. \tag{4.12}$$

A natural choice for $\mathcal{DH}(x,u^h)$ is

$$\mathcal{DH}\left(x,u^h\right)=\int_0^1 D_{\mathbf{p}}H\left(x,u^h,sDu^h+(1-s)p^{\text{ref}}\right)ds \tag{4.13}$$

and then, instead of (4.8), we consider the numerical Hamiltonian and the Hamiltonian

(4.14)

$$\begin{aligned}&\mathcal{H}_\sigma\left(\sigma,u_\sigma,u_{\xi\,\xi\in\mathcal{V}_\sigma}\right)\\&\quad:=\left(\int_\Omega H\left(\sigma,Du^h\right)\mathcal{N}_\sigma dx+h\int_\Omega\left[\frac{\mathcal{DH}\left(\sigma,Du^h\right)}{\|\mathcal{DH}(\sigma,Du^h)\|}\cdot D\mathcal{N}_\sigma\right]\,H\left(\sigma,Du^h\right)dx\right)\\&\qquad\times\left(\int_\Omega\mathcal{N}_\sigma dx\right)^{-1},\end{aligned}$$

where p^{ref} is an arbitrary vector. Note that the accuracy arguments of the previous paragraph still hold, as well as Lemma 4.1.

Implementation details. We end this section by giving some details about the implementation of (4.8). We follow [15]. From (4.8), we see that the numerator and the denominator can be computed following an element-based approach. In pseudocode, this gives

1. initialize $\mathcal{H}_\sigma=0$ and $\psi_\sigma=0$ for any degree of freedom;
2. loop over elements T, $j_t=1,\dots,n_e$
   (a) compute $\mathcal{N}_\sigma$ for each degree of freedom on T,
   (b) compute u and Du,
   (c) evaluate

$$\begin{aligned}\mathcal{H}_\sigma=\mathcal{H}_\sigma&+\int_T H\left(x,u^h,Du^h\right)\mathcal{N}_\sigma dx\\&+h\int_T\frac{\mathcal{DH}\left(x,u^h\right)}{\|\mathcal{DH}\left(x,u^h\right)\|}\cdot D\mathcal{N}_\sigma\;D_pH\left(x,u^h,Du^h\right)\cdot Du^h dx\end{aligned}$$

   via high order quadrature formula and thanks to (4.13),
   (d) evaluate

$$\psi_\sigma=\omega_\sigma+\int_T\mathcal{N}_\sigma dx$$

   via high order quadrature formula;

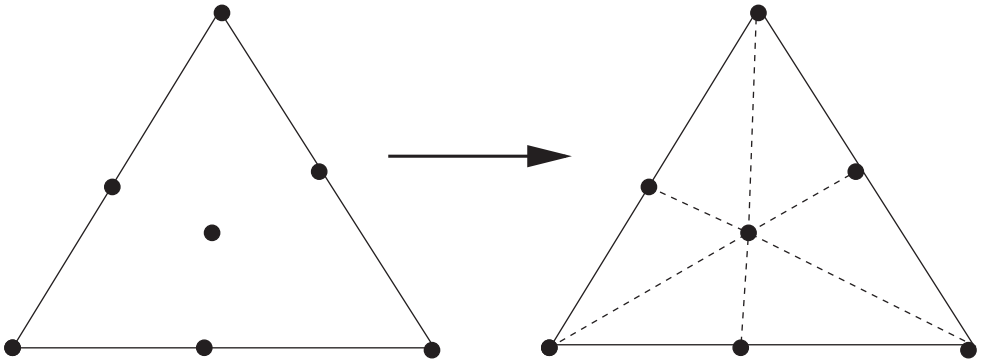

FIG. 4.5. *Subtriangulation used for the low order schemes.*

3. compute

$$\mathcal{H}_\sigma = \frac{\mathcal{H}_\sigma}{\psi_\sigma}.$$

Remark 5. When implementing the blended scheme (2.12a), the low order Hamiltonians are implemented by using a subtriangulation. In the case of $\widetilde{\mathbb{P}^2(T)}$, we use the subtriangulation of Figure 4.5.

4.3. Practical implementation of the scheme (2.12)–(2.13)–(2.10). The most straightforward implementation is to use the pseudotime-inconsistent scheme like

$$u_\sigma^{n+1} = u_\sigma^n - \Delta t \mathcal{H}_\sigma,$$

where the time step is limited by a CFL-type condition. Since we are computing *steady* solution, the time step and the time t_n are only relaxation and iterative parameters. Hence, a better strategy is to use a local time step.

Remember, we are using the limiter (2.10); it is useful to see exactly how the scheme is written. Following the notations of section (2), we see that if $\alpha_- = 1$,

- if $r > \beta + \dfrac{1}{\alpha_+}$, $\mathcal{H}_\sigma = \gamma \mathcal{H}_\sigma^H$, with $\gamma = \dfrac{1}{\beta} \leq 1$ if $\beta \geq 0$;
- if $r \in \left[\beta, \beta + \dfrac{1}{\alpha_+}\right]$, $\mathcal{H}_\sigma = \gamma \mathcal{H}_\sigma^H$, with $\gamma = 1 + \alpha_+ \dfrac{(1-r)(r-\beta)}{r} \in [0,1]$ if $\beta \geq 1$;
- if $r \in [0, \beta]$, $\mathcal{H}_\sigma = \mathcal{H}_\sigma^H$;
- if $r \in [-1, 0]$, $\mathcal{H}_\sigma = \gamma \mathcal{H}_\sigma^H$, with $\gamma = -\dfrac{\mathcal{H}_\sigma^H}{\mathcal{H}_\sigma^M} \in [0,1]$;
- if $r < -\dfrac{1}{\alpha_-}$, $\mathcal{H}_\sigma = \mathcal{H}_\sigma^M$.

Thus, we see that if $\beta \geq 1$ and $\alpha_- = 1$, we can always write $\mathcal{H}_\sigma = \mathcal{H}^H$ or $\mathcal{H}_\sigma = \gamma \mathcal{H}_\sigma^H$, with $\sigma \in [0,1]$. The scheme, omitting the boundary conditions, is written as

$$u_\sigma^{n+1} = u_\sigma^n - \Delta t \gamma(u^n)_\sigma \begin{cases} \mathcal{H}_\sigma^M & \text{if } r \leq -1, \\ \mathcal{H}_\sigma^H & \text{if } r \geq -1, \end{cases} - \Delta t \times \varepsilon(h),$$

with $0 \leq \gamma(u^n) \leq 1$. This leads to the following choice of the local time step:

$\Delta t_\sigma := \Delta t \gamma(u^n)_\sigma$. The optimal stability condition is

$$\Delta t_\sigma = CFL \times \begin{cases} \Delta t^L_{\max} & \text{if } r \le -1, \\ \Delta t^H_{\max} & \text{if } r \ge -1, \end{cases} \tag{4.15}$$

where $\Delta t^L_{\max}$ (resp. $\Delta t^H_{\max}$) is the maximum time step allowed by the first order scheme (resp. the high order scheme).

Hence, in practice, we implement the following scheme (using the fact that $\varepsilon(h) = Ch^k$, with $C > 0$ arbitrary, so we can redefine ε):

1. For an internal degree of freedom,

$$u^{n+1}_\sigma = u^n_\sigma - \Delta t_\sigma \mathcal{H}_\sigma, \tag{4.16}$$

where

$$\mathcal{H}_\sigma = \begin{cases} \mathcal{H}^M_\sigma + \varepsilon(h) & \text{if } r \le -1, \\ \mathcal{H}^H_\sigma + \varepsilon(h) & \text{else.} \end{cases} \tag{4.17}$$

2. For a degree of freedom on the boundary, u^{n+1}_σ is defined as the solution of

$$\max\left(\frac{u^{n+1}_\sigma - u^n_\sigma}{\Delta t_\sigma} + \mathcal{H}^L_\sigma, u^{n+1}_\sigma - g(\sigma) \right) = 0, \tag{4.18}$$

with $\Delta t_\sigma = CFL \times \Delta t^L_{\max}$.

We see that, thanks to the local time stepping strategy, we can use almost everywhere the high order unlimited scheme, without creating spurious oscillations in the solution. In order to illustrate this remark, and the way we have defined the various schemes throughout the paper, we provide now some numerical illustrations.

5. Numerical illustrations.

5.1. Computational strategy. If $\varepsilon(h) = 0$, a close examination of (2.2) and (2.8) reveals that if one initializes the calculation with a *converged* first order solution (resp. a *converged* second order solution), we get $\ell = 1$ (resp. $\ell = 0$) in general. In other words, the high order scheme will provide either a first order solution or a second order solution possibly with oscillations! The role of the parameter $\varepsilon(h) \neq 0$ is precisely to avoid this situation.

In practice, either we initialize by a constant function and we run the high order scheme from scratch. This strategy works well for the one-dimensional examples below because there is no particular difficulties in the evaluation of H. In the two-dimensional cases, because a $D_{\mathbf{p}}H$ (resp. $\mathcal{DH}$) appears in the denominator of (4.8) (resp. (4.14)), we have to first run the first order scheme up to a point where there is no difficulty in the evaluation of $\mathcal{H}^H$, and then we run the high order schemes.

Except in subsection 5.3.2 where $\widetilde{\mathbb{P}^2(T)}$ is used, the interpolation is always in $\mathbb{P}^1(T)$.

5.2. One-dimensional examples. In this example, we consider the Lax–Friedrichs scheme and the one-dimensional version of the high order schemes (4.8) and (4.14). The test problem is

$$\begin{aligned} &|u'| - n(x) = 0 \qquad x \in [0,1], \\ &u(0) = u(1) = 0, \end{aligned} \tag{5.1}$$

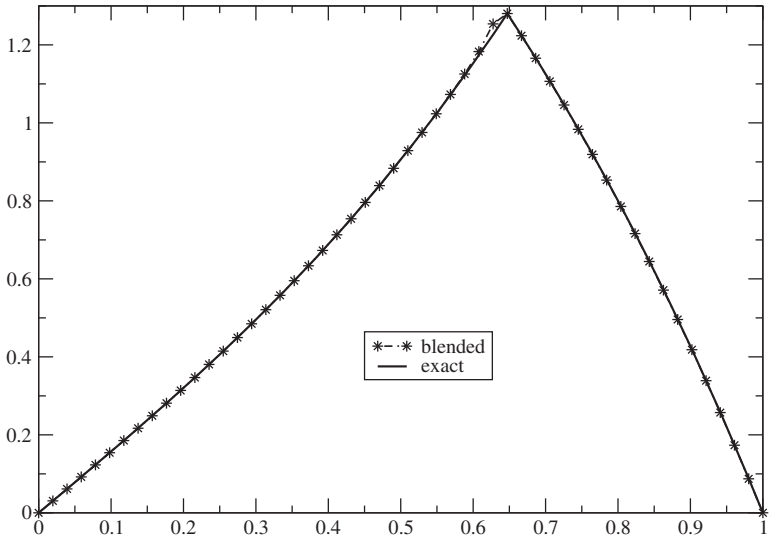

FIG. 5.1. *Problem* (5.1)*: exact solution and solution obtained by the blended scheme,* 50 *mesh points.*

where $n(x) = 3x^2 + a$, with $a = \frac{1-2x_0^3}{2x_0-1}$ and $x_0 = \frac{\sqrt[3]{2}+2}{4\sqrt[3]{2}}$. The solution is

$$u(x) = \begin{cases} x^3 + ax & \text{if } x \in [0, x_0], \\ 1 + a - ax - x^3 & \text{if } x \in [x_0, 1]. \end{cases}$$

In this example, the solution is computed by a blending between the first order Lax–Friedrichs scheme and the compact scheme of section 4.2.2 adapted to the one-dimensional case. The scheme should be formally second order accurate. Since the Hamiltonian $x \mapsto |x|$ is homogeneous of degree 1, we use the original formula of [15].

We have represented the solution on Figure 5.1 for only 50 mesh points as well as zooms in $[0.4, 0.6]$ where the solution is smooth (see Figure 5.2) and around the maximum (see Figure 5.3).

We have also computed the L^1 error in $[0, 1]$ (Figure 5.4) and L^∞ error in $[\frac{1}{\sqrt[3]{2}}, \frac{1}{2}]$ where the solution is still smooth (Figure 5.4). We see that the expected order of accuracy is obtained. The convergence behavior of the blended scheme seems better than those of the unlimited second order scheme.

Then we consider an inhomogeneous and nonconvex Hamiltonian, namely,

$$H(x, p) = \cos(p)^2 + |p|.$$

The problem reads

$$H(x, u') = 0 \text{ in } x \in [0, 1], \text{with } u(0) = u(1) = 0.$$

On Figure 5.5, we display H in the range $x \in [-1, 1]$. The numerical solutions are displayed in Figure 5.6 in the range $x \in [0.5, 0.8]$. The mesh has 50 points. We have numerically checked that the gradient of the solution may be larger than 1 in absolute value, so that nonconvex effects do occur. We have chosen $p_{ref} = 0$ in the one-dimensional version of (4.14).

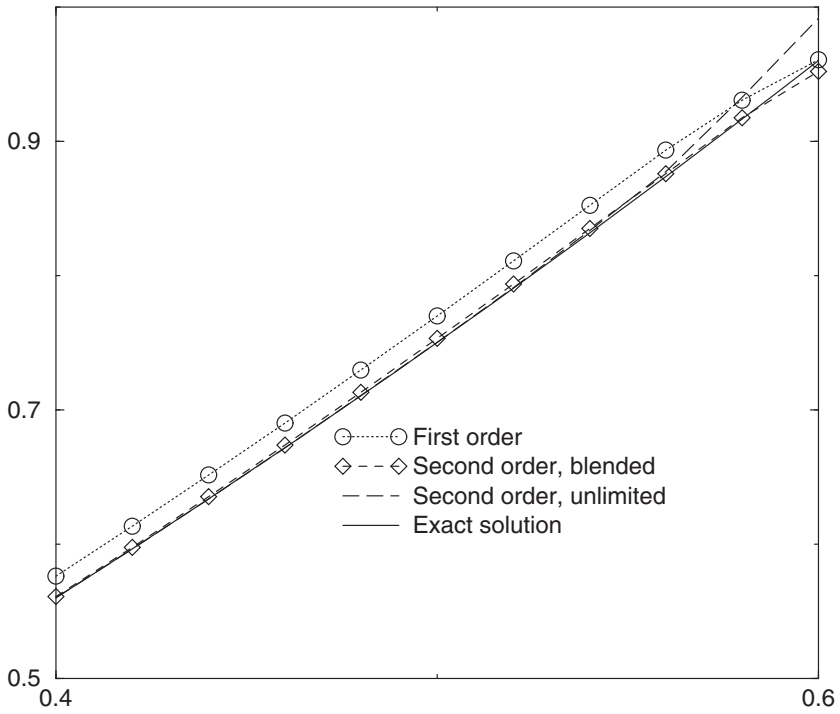

FIG. 5.2. *Zoom in* $[0.4, 0.6]$ *for* (5.1).

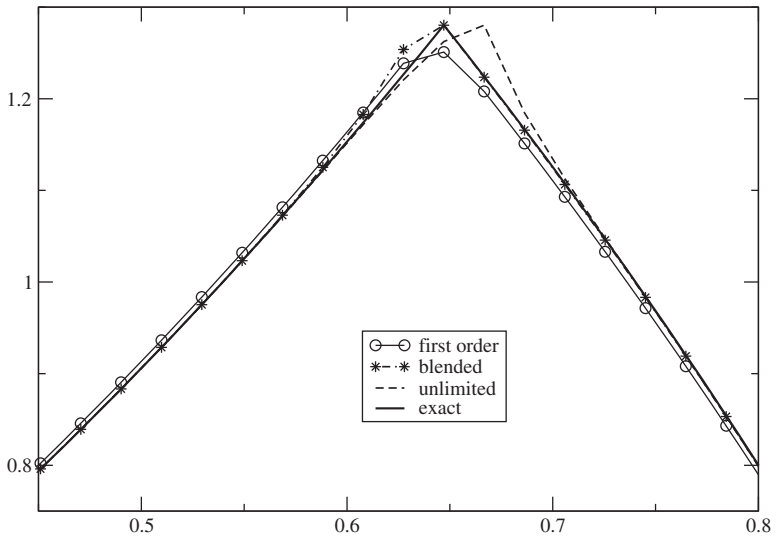

FIG. 5.3. *Zoom around the maximum for* (5.1).

The iterative convergence has been run to machine accuracy. Once again, the blended solution lies between the first order and second order unlimited solution. In the smooth regions, the two second order solutions are indistinguishable, while at the extrema, the quality of the first order and blended solutions are comparable. We note an overshoot for the second order unlimited solution.

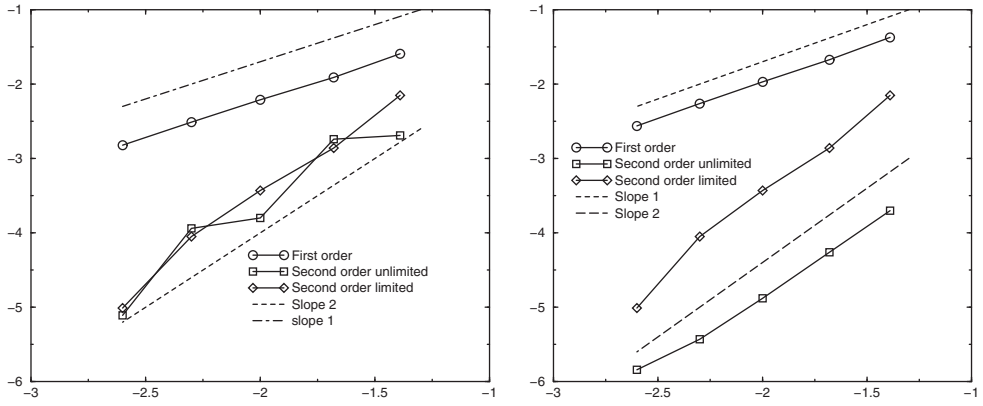

L^1 norm L^∞ norm

FIG. 5.4. *Error in the L^1 and L^∞ norm for the first order, blended, and second order unlimited scheme. The error in the L^∞ norm is evaluated in $[1/\sqrt[3]{2}, 1/2]$. The slope -1 and -2 are represented.*

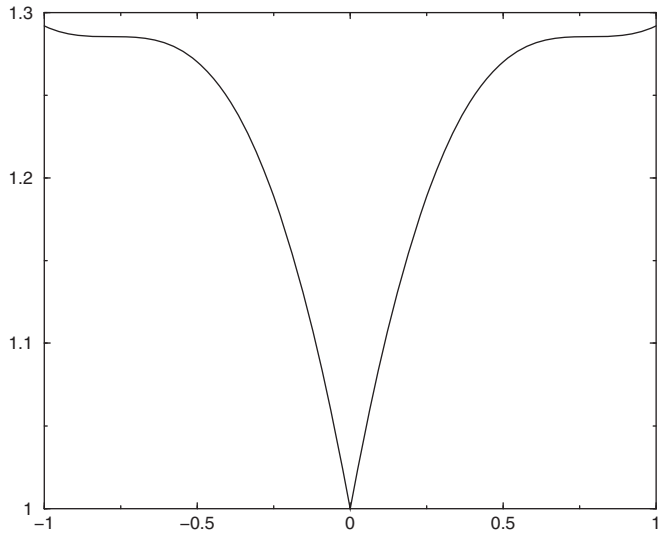

FIG. 5.5. *Plot of $H(p) = \cos(p)^2 + |p|$ in $x \in [-1, 1]$.*

5.3. Two-dimensional examples. First, we consider an example of a homogeneous Hamiltonian (the Eikonal Hamiltonian) and second, an inhomogeneous but still convex one. We have not considered any nonconvex case, since it seems difficult to construct an example for which existence and uniqueness, with Dirichlet boundary conditions, can be proved, at least from the information provided in [1].

5.3.1. Eikonal equation. We consider the Eikonal equation with a Dirichlet boundary condition on the inner boundary of the geometry considered in Figure 5.7 The solution is nothing more than the distance function to this boundary. On Figure 5.8, we superimpose the first order solution, the second order unlimited solution, and the limited one. This figure shows that the two second order solutions superimpose in the area where the solution is smooth, that the unlimited exhibits slight oscillations as expected. They are totally cured by the limitation procedure.

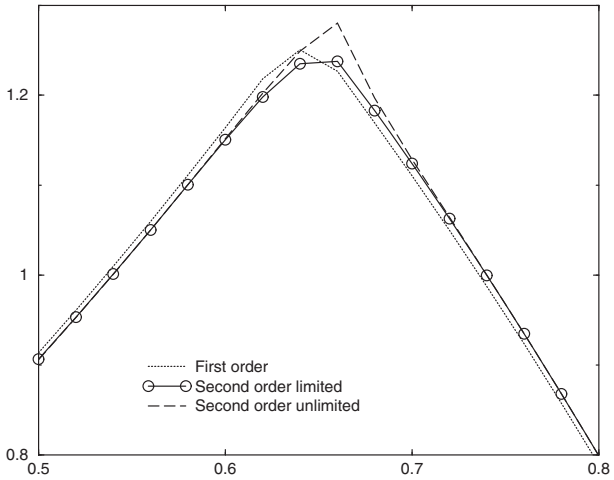

FIG. 5.6. *Plot of the first order, second order, and blended solutions in* $x \in [0.5, 0.8]$.

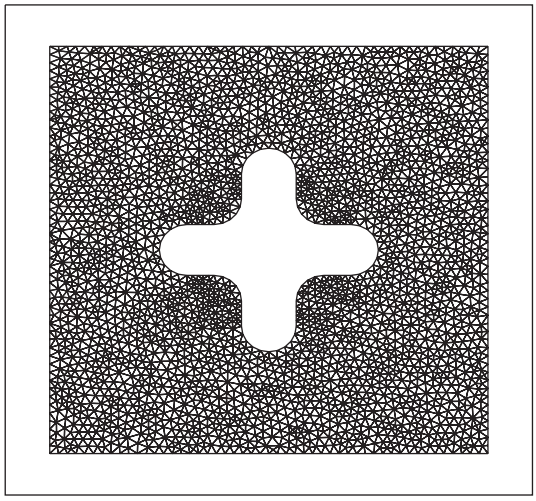

FIG. 5.7. *Mesh and geometry for the two-dimensional example.*

5.3.2. Inhomogeneous case. The problem is to find u in $\Omega = [0,1]\times[0,1] - C$, where $C = \{(x,y) \in [0,1/2]\times[0,1/2]$ and $(x-1/2)^2 + (y-1/2)^2 \geq 1\}$, solution of

$$\psi(Du) - 1 = 0 \text{ in } \Omega \text{ and } u = 0 \text{ on } \partial\Omega. \tag{5.2}$$

In (5.2), ψ is defined as

$$\psi(p) = \begin{cases} \dfrac{\|p\|^2 + 1}{2} & \text{if } \|p\| \leq 1, \\ \|p\| & \text{else.} \end{cases}$$

In that case, the third order accurate interpolant of [22] is used; see section 4.2, yielding a formally third order accurate solution. Our purpose is not to check a third order accurate error behavior but to show that other interpolation techniques are

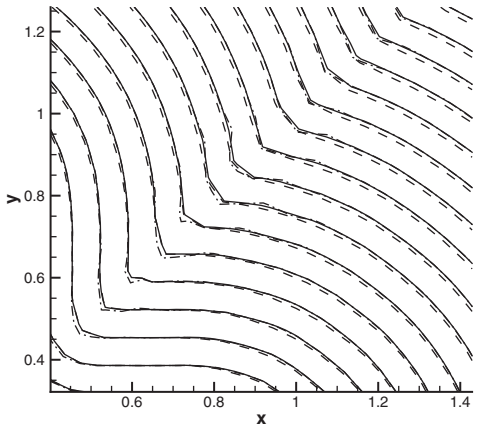

FIG. 5.8. *First order solution (dashed lines), second order unlimited solution (dash-dotted lines), and second order limited solution (plain lines lines).*

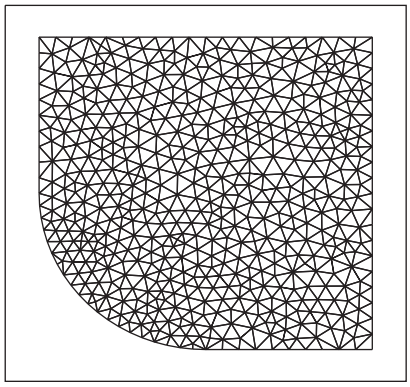

FIG. 5.9. *Mesh for the inhomogeneous test case. Only the vertices of the mesh are displayed; the other degrees of freedom (midpoint of edges and centroids) are omitted.*

possible, and the resulting scheme is still simple to implement. The vector $\mathcal{DH}$ is chosen to be $\frac{Du^h}{||Du^h||}$ as in the homogeneous case because $\psi' \geq 0$. The mesh is very crude; see Figure 5.9.

In Figure 5.10, we have plotted the first order (Lax–Friedrich), the second order unlimited, and the blended solution. On Figure 5.10 we have plotted the solution of *all* the degrees of freedom.

First, we see a very clear improvement of the solution between the first order and higher order solution. The resolution of discontinuities is very sharp.

The second order solution is already very good. We have small wiggles or what look like small wiggles.

Remark 6 (does the boundary condition spoil the accuracy?). One of the referees has pointed out the question whether the effective accuracy is governed by the accuracy at the boundary. At least in the case of convex (at the boundary) Hamiltonians and with the Godunov boundary Hamiltonian as in all the numerical examples of this paper, this is not the case. The reason is the following. At a boundary, except perhaps at exceptional points, either the characteristics of the steady problems (1.1)

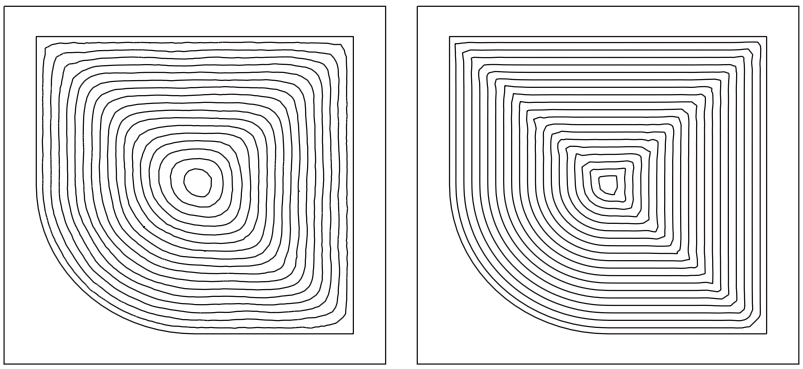

First order, $u \in [0, 0.4364]$ Second order, $u \in [0, 0.4922]$

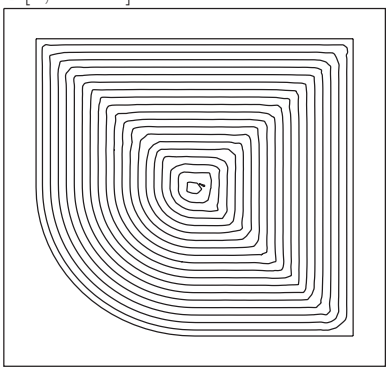

Blended solution, $u \in [0.4848]$

FIG. 5.10. *Solution displayed on the vertices of the mesh of Figure* 5.9.

are ingoing or outgoing. If they are ingoing, because the Hamiltonian is convex and because of the choice of the boundary Hamiltiona, our BCs amount to impose strongly the boundary condition. This is a simple convexity argument. If the characteristics are outgoing, then the boundary Hamiltonian plays no role. If we had taken Neumann boundary, then the situation is simpler since we can impose strongly the boundary condition, and the question becomes that of how accurate we are to approximate the normal derivative; see [19]. Hence the accuracy at the boundary cannot be spoiled.

6. Conclusion, further work. In this paper, we have presented a general and simple method for increasing the order of accuracy of schemes for first order Hamilton–Jacobi equations. It relies on a simple blending of a low order and a high order scheme. The structure of the blending has been studied so that the original stability properties of the original first order scheme are kept. The main difficulty is to construct high order schemes that are stable in a meaning too precise. We have presented some examples, but our examples are clearly not optimal.

This work can be extended in two directions. The first one is about the construction of better high order schemes. There is lots of flexibility in the construction: the only constraint is the consistency of the high order scheme; there is no conservation-related constraints as for conservation equations, since these constraints are meaningless. Due to the generality of our method, we can adapt it of blended low order schemes and discontinuous Galerkin-like schemes such as those of [14, 20]. This will be done in a future work.

The second direction is about unsteady problems. Consider

$$\frac{\partial u}{\partial t} + H(x, u, Du) = 0.$$

We can prediscretize it in time first, for example, by doing

$$\frac{3}{2}\left(u^{n+1} - u^n\right) - \frac{1}{2}\left(u^n - u^{n-1}\right) + \Delta t H\left(x, u^{n+1}, Du^{n+1}\right) = 0,$$

which is a second order in time approximation of the true problem. This equation can be seen as a steady Hamilton–Jacobi problem in the variable $v := u^{n+1}$. Other, and more accurate prediscretization, leading to problems like

$$\alpha u^{n+1} + \beta \Delta t H\left(x, u^{n+1}, Du^{n+1}\right) = F\left(\left\{u^k, k = n, n-1, \ldots, n-p\right\}\right) \equiv F(x),$$

with $\alpha, \beta > 0$ and for p integer, exist. Because our technique needs *only* the consistency of the Hamiltonian, it can be applied in this context and will lead to high order accuracy in space and time schemes. This will also be investigated in future research.

Acknowledgments. This research has been motivated by S. Ballereau from SME, France. I would also like to thank the three unknown referees whose sharp comments have led to a drastic improvement of the paper.

REFERENCES

[1] G. Barles, *Solutions de Viscosité des équations de Hamilton–Jacobi*, Math. Appl. (Berlin), Vol. 17, Springer-Verlag, Berlin, 1994.
[2] M. Teillaud, *Toward Dynamic Randomized Algorithms in Computational Geometry*, Lecture Notes in Comput. Sci. 758, Springer-Verlag, Berlin, 1993.
[3] G. Barles and P.E. Souganidis, *Convergence of approximation schemes for fully nonlinear second order equations*, Asymptot. Anal., 4 (1991), pp. 271–283.
[4] E. Rouy and A. Tourin, *A viscosity solutions approach to shape-from-shading*, SIAM J. Numer. Anal., 29 (1992), pp. 867–884.
[5] J.A. Sethian and A. Vladimirsky, *Ordered upwind methods for static Hamilton-Jacobi equations*, Proc. Natl. Acad. Sci. USA, 98 (2001), pp. 11069–11074.
[6] S. Osher and C.-W. Shu, *High-order essentially nonoscillatory schemes for Hamilton–Jacobi equations*, SIAM J. Numer. Anal., 28 (1991), pp. 907–922.
[7] C. Kao, S. Osher, and J. Qian, *Lax-Friedrichs sweeping scheme for static Hamilton-Jacobi equations*, J. Comput. Phys., 196 (2004), pp. 367–391.
[8] C. Kao, S. Osher, and Y. Tsai, *Fast sweeping methods for static Hamilton–Jacobi equations*, SIAM J. Numer. Anal., 42 (2005), pp. 2612–2632.
[9] M.G. Crandall and P.-L. Lions, *Two approximations of solutions of Hamilton–Jacobi equations*, Math. Comp., 43 (1984), pp. 1–19.
[10] M. Bardi and S. Osher, *The nonconvex multidimensional Riemann problem for Hamilton–Jacobi equations*, SIAM J. Math. Anal., 22 (1991), pp. 344–351.
[11] A. Kurganov and E. Tadmor, *New high-resolution semi-discrete central schemes for Hamilton-Jacobi equations*, J. Comput. Phys., 160 (2000), pp. 720–742.
[12] S. Bryson, A. Kurganov, D. Levy, and G. Petrova, *Semi-discrete central-upwind schemes with reduced dissipation for Hamilton-Jacobi equations*, IMA J. Numer. Anal., 25 (2005), pp. 113–138.
[13] R. Abgrall, *Numerical discretization of first order Hamilton–Jacobi equations on triangular meshes*, Comm. Pure Appl. Math., XLIX (1996), pp. 1339–1373.
[14] C. Hu and C.W. Shu, *A discontinuous Galerkin finite element method for Hamilton–Jacobi equations*, SIAM J. Sci. Comput., 21 (1999), pp. 666–690.
[15] T.J. Barth and J.A. Sethian, *Numerical schemes for the Hamilton–Jacobi and level set equations on triangulated domains*, J. Comput. Phys., 145 (1998), pp. 1–40.
[16] D. Levy, S. Nayak, C.-W. Shu, and Y.-T. Zhang, *Central WENO schemes for Hamilton-Jacobi equations on triangular meshes*, SIAM J. Sci. Comput., 28 (2006), pp. 2229–2247.

[17] P. E. Souganidis, *Approximation schemes for viscosity solutions of Hamilton-Jacobi equations*, J. Differential Equations, 59 (1985), pp. 1–43.
[18] C.-T. Lin and E. Tadmor, *L^1-stability and error estimates for approximate Hamilton-Jacobi solutions*, Numer. Math., 87 (2001), pp. 701–735.
[19] R. Abgrall, *Numerical discretization of boundary conditions for first order Hamilton–Jacobi equations*, SIAM J. Numer. Anal., 41 (2003), pp. 2233–2261.
[20] F. Li and C.-W. Shu, *Reinterpretation and simplified implementation of a discontinuous Galerkin method for Hamilton–Jacobi equations*, Appl. Math. Lett., 18 (2005), pp. 1204–1209.
[21] A. Harten, B. Engquist, S. Osher, and S. R. Chakravarthy, *Uniformly high order accurate essentially non-oscillatory schemes.* III. *(Reprint).* J. Comput. Phys., 131 (1997), pp. 3–47.
[22] G. Cohen, P. Joly, J.E. Roberts, and N. Tordjman, *Higher order triangular finite elements with mass lumping for the wave equation*, SIAM J. Numer. Anal., 38 (2001), pp. 2047–2078.
[23] A. Kurganov and G. Petrova, *Central-upwind schemes on triangular grids for hyperbolic systems of conservation laws*, Numer. Methods Partial Differential Equations, 21 (2005), pp. 536–552.
[24] T.J.R. Hughes, L.P. Franca, and M. Mallet, *Finite element formulation for computational fluid dynamics:* I *symmetric forms of the compressible Euler and Navier Stokes equations and the second law of thermodynamics*, Comput. Methods Appl. Mech. Engrg., 54 (1986), pp. 223–234.